Cellular/Molecular

Distinct Regulation of β2 and β3 Subunit-Containing Cerebellar Synaptic $GABA_A$ Receptors by Calcium/Calmodulin-Dependent Protein Kinase II

Catriona M. Houston, Alastair M. Hosie, and Trevor G. Smart
Department of Pharmacology, University College London, London WC1E 6BT, United Kingdom

Modulation of $GABA_A$ receptor function and inhibitory synaptic transmission by phosphorylation has profound consequences for the control of synaptic plasticity and network excitability. We have established that activating α-calcium/calmodulin-dependent protein kinase II (α-CaMK-II) in cerebellar granule neurons differentially affects populations of IPSCs that correspond to $GABA_A$ receptors containing different subtypes of β subunit. By using transgenic mice, we ascertained that α-CaMK-II increased IPSC amplitude but not the decay time by acting via β2 subunit-containing $GABA_A$ receptors. In contrast, IPSC populations whose decay times were increased by α-CaMK-II were most likely mediated by β3 subunit-containing receptors. Expressing α-CaMK-II with mutations that affected kinase function revealed that Ca^{2+} and calmodulin binding is crucial for α-CaMK-II modulation of $GABA_A$ receptors, whereas kinase autophosphorylation is not. These findings have significant consequences for understanding the role of synaptic $GABA_A$ receptor heterogeneity within neurons and the precise regulation of inhibitory transmission by CaMK-II phosphorylation.

Key words: **$GABA_A$ receptor; CaMK-II; β2 subunit; β3 subunit; synaptic inhibition; phosphorylation**

Introduction

Phosphorylation of $GABA_A$ receptors is an important endogenous mechanism for exerting either short- or long-term regulation of inhibitory synaptic transmission (Moss and Smart, 1996; Brandon et al., 2002; Lüscher and Keller, 2004). Phosphorylation covalently modifies receptor structure, which can alter $GABA_A$ receptor ion channel properties, such as desensitization (Jones and Westbrook, 1997) or channel open probability (Moss et al., 1995), as well as affecting receptor trafficking to and from inhibitory synapses. By dynamically modulating the numbers of synaptic receptors, phosphorylation will have an important influence on inhibitory synaptic efficacy and synaptic plasticity (Kittler and Moss, 2003; Wang et al., 2003).

Previous studies have revealed that regulation of receptor function by phosphorylation exhibits considerable diversity. For $GABA_A$ receptors, this is manifest by protein kinases differentially affecting particular receptor isoforms (McDonald et al., 1998), by the modification of receptor function by phosphorylation depending on the protein kinase involved (Poisbeau et al., 1999), and by the influence of different cell types on the regulation by protein kinases (Nusser et al., 1999).

One protein kinase that has a profound impact on fast GABA-mediated synaptic inhibition is calcium/calmodulin-dependent protein kinase II (CaMK-II). The application of preactivated α-CaMK-II to hippocampal CA1 neurons increased the amplitudes of evoked IPSPs and reduced receptor desensitization (Wang et al., 1995). Internal application of preactivated α-CaMK-II into Purkinje neurons also increased the amplitude of miniature IPSCs (mIPSCs) without affecting their decay time constants (Kano et al., 1996). These functional studies strongly suggested that the $GABA_A$ receptor is a substrate for CaMK-II. Indeed, previous and subsequent biochemical studies have demonstrated that CaMK-II phosphorylates the large intracellular domains of β and γ subunits of the $GABA_A$ receptor when they are expressed as GST-fusion proteins (McDonald and Moss, 1994, 1997). Furthermore, when recombinant $GABA_A$ receptors are expressed in NG108-15 cells and cultured cerebellar granule neurons, α-CaMK-II had a differential effect on the amplitudes of whole-cell GABA-activated currents depending on whether the $GABA_A$ receptors were assembled with β2 or β3 subunits. The amplitudes of GABA-activated currents mediated by α1β3γ2S receptors were increased by α-CaMK-II, whereas currents mediated by α1β2γ2S receptors remained unaffected (Houston and Smart, 2006). It therefore followed that CaMK-II could differentially affect inhibitory synaptic transmission, particularly at synapses at which the β subunit composition of the synaptic $GABA_A$ receptors might vary.

In this study, we report that activating α-CaMK-II in cerebellar granule neurons significantly altered inhibitory synaptic transmission by modulating the amplitudes and decay times of spontaneous IPSCs (sIPSCs). This modulation required the binding of Ca^{2+} and calmodulin (CaM) to the kinase, but autophosphorylation of CaMK-II was not crucial for the regulation of $GABA_A$ receptor function. CaMK-II caused a differential modu-

Received Dec. 14, 2007; revised April 22, 2008; accepted June 5, 2008.

This work was supported by the Medical Research Council and The Wellcome Trust. We thank Helena da Silva for site-directed mutagenesis of α-CaMK-II and Paul Whiting for the β2 knock-out mice. We are grateful to Phil Thomas for critical comments on this manuscript.

Correspondence should be addressed to Prof. Trevor G. Smart, Department of Pharmacology, University College London, Gower Street, London WC1E 6BT, UK. E-mail: t.smart@ucl.ac.uk.

DOI:10.1523/JNEUROSCI.5531-07.2008

 0270-6474/08/287574-11$15.00/0

lation of inhibitory synaptic currents, which corresponded to synapses containing β2 and β3 subunit-containing receptors. This indicates that CaMK-II can differentially modulate the function of specific inhibitory synapses depending on the β subunit composition of the synaptic $GABA_A$ receptors. This is likely to have important consequences for the control of neuronal excitability.

Materials and Methods

Cell culture. Dissociated cerebellar cultures were prepared as follows: the cerebellum was removed from postnatal day 1 (P1) Sprague Dawley rats and incubated in 0.1% (w/v) trypsin (Sigma-Aldrich) for 10 min. Trypsin activity was quenched by washing (three times) in HBSS. The tissue was then triturated in DNase [Sigma-Aldrich; 0.05% (w/v) in 12 mM $MgSO_4$] using flame-polished Pasteur pipettes of decreasing bore diameters. Cells were plated at a density of 5×10^6 cells/ml on glass coverslips, previously coated in poly-L-ornithine (Sigma-Aldrich; 500 μg/ml) and maintained in culture for 7–10 d *in vitro* (DIV) in BME (5 mM KCl; Invitrogen) supplemented with 0.5% (w/v) glucose, 5 mg/L insulin, 5 mg/L transferrin, 5 mg/L selenium (Sigma-Aldrich), 20 U/ml penicillin G and 20 μg/ml streptomycin, 0.2 mM glutamine, 1.2 mM NaCl, and 5% (v/v) fetal calf serum. All procedures involving animals were conducted according to the requirements of the United Kingdom Home Office Animals (Scientific Procedures) Act 1986.

cDNA constructs and transfection. Rat α-CaMK-II cDNA in the plasmid vector pcDNA3 was mutated by site-directed mutagenesis to form α-CaMK-II T286D, T286A, A302R, and K42R cDNAs. Cerebellar granule cells (CGCs) were transfected at 5–6 DIV using Effectene (QIAGEN) in the presence of 0.3–0.5 μg of total cDNA per dish, with α-CaMK-II and enhanced green fluorescent protein (EGFP) cDNAs present in equal ratio.

Patch-clamp electrophysiology. Whole-cell membrane currents were recorded from single cells with an Axopatch 1C amplifier or the MultiClamp 700A (Molecular Devices). Patch pipettes (8–9 MΩ) were filled with a solution containing the following (in mM): 150 CsCl, 1 $MgCl_2$, 10 HEPES, 4 Na_2ATP, 0.1 $CaCl_2$, and 1.1 mM EGTA, pH adjusted to 7.2 with 1 M CsOH (290–310 mOsm). The cells were perfused with Krebs' solution containing the following (in mM): 140 NaCl, 4.7 KCl, 1.2 $MgCl_2$, 2.52 $CaCl_2$, 11 D-glucose, 5 HEPES adjusted to pH 7.4 with 1 M NaOH (290–310 mOsm). Currents were filtered at 3 kHz (eight-pole Bessel filter) and analyzed using Clampex 8.2 (Molecular Devices). Cells were not used for analysis if their access or series resistances changed by >15%. All experiments were performed at room temperature (25°C). Cells were continuously perfused with CNQX (10 μM), AP-5 (20 μM), and the internal patch pipette solution contained 5 mM lidocaine *N*-triethyl bromide (QX-314). Recordings of sIPSCs started 5 min after achieving the whole-cell configuration.

Preparation of α-CaMK-II. Purified recombinant α-CaMK-II (New England Biolabs) was preactivated (Houston and Smart, 2006; Houston et al., 2007) by incubation with 1.2 μM CaM, 1.5 mM $CaCl_2$, and 0.4 mM ATP-γ-S for 15 min at 25°C, to promote Ca^{2+}/CaM binding and subsequent autophosphorylation at Thr^{286} (resulting in Ca^{2+}-independent activity). α-CaMK-II was diluted with patch pipette solution to give a final concentration of 85 nM. Control recordings used the same autophosphorylation buffer, diluted appropriately, but without α-CaMK-II. The specific CaMK-II inhibitory peptide, CaMK-II-Ntide (Merck) (Chang et al., 1998), was included in the patch pipette solution at a concentration of 1 μM. Control recordings used a scrambled version of this peptide (1 μM; Cambridge Peptides).

$GABA_A$ receptor β2 subunit knock-out mouse. Mouse cerebellar granule cell cultures were created using P0–P2 mice from β2 knock-out (−/−) and wild-type (wt) mouse strains (Merck Sharp & Dohme). These strains were created by deletion of exons 6 and 7 of the β2 gene by homologous recombination. Heterozygous F_3 generation mice were crossbred to produce $\beta 2^{-/-}$ and wt strains of 50% C57BL/6, 50% 129SvEv genetic background (Sur et al., 2001). F_6–F_7 generation mice were used in the current experiments and the genotype of these mice was confirmed by PCR.

Immunocytochemistry of $GABA_A$ receptor subunits. Cerebellar granule cell cultures [maintained in 5% (v/v) horse serum] were fixed in 4% paraformaldehyde quenched with 50 mM NH_4Cl. After permeabilization (0.1% Triton X; 8 min), the cells were incubated for 1 h with the first primary antibody (rabbit anti-β3; 1:100; Millipore) and for 1 h with AffiniPure Fab Fragment goat anti-rabbit (Jackson ImmunoResearch) followed by a 45 min incubation with donkey anti-goat Rhodamine Red-X (1:75; Jackson ImmunoResearch). The cells were then incubated for 1 h with the second set of primary antibodies [rabbit anti-β2; 1:50 (W. Sieghart, University of Vienna, Vienna, Austria); mouse anti-GAD; 1:100; Roche] and for 45 min with the secondary antibodies (donkey anti-mouse Cy5, 1:50; donkey anti-rabbit Cy2, 1:75; Jackson ImmunoResearch). This protocol enabled us to use two primary antibodies raised in the same host species; however, we also obtained images using antibodies raised in different species involving a 1 h incubation with the primary antibodies [goat anti-β3, 1:150 (Santa Cruz Biotechnology); mouse anti-GAD, 1:100 (Roche); and either rabbit anti-β1, 1:50, or rabbit anti-β2, 1:50 (W. Sieghart)] and a 45 min incubation with the secondary antibodies (donkey anti-goat Rhodamine Red-X, 1:75; donkey anti-mouse Cy5, 1:50; and donkey anti-rabbit FITC, 1:50; Jackson ImmunoResearch). Immunofluorescent images were acquired using the Carl Zeiss 510 Meta confocal microscope equipped with argon (488 nm) and helium–neon lasers (543 and 633 nm), with a 40× objective (Houston and Smart, 2006; Houston et al., 2007). Each image was acquired as a 1 μm optical slice for each channel. Images were threshold adjusted and the number of puncta determined using NIH Image J software. The number of puncta were verified by eye and densities calculated as puncta per micrometer length of dendrite.

Analysis of IPSC decay time constants. Within MiniAnalysis (version 6.0.1; Synaptosoft), synaptic currents were detected automatically with an amplitude threshold of 5–8 pA. Each event was then manually assessed for its inclusion in the analysis. Mean values were calculated for the frequency, peak amplitude, and half-widths (time taken to decay to 50% of the peak amplitude) over the period of recording. Synaptic events were chosen for additional analysis of their decay time constants if there were no deflections in their rising or decaying phases and they decayed back to the baseline holding current. Events of low amplitude (<5 pA) were discarded from this analysis because they were thought to represent events occurring at the most distant synapses and therefore more likely to be affected by dendritic filtering or cabling. Only cells lacking any clear correlation between IPSC rise time and amplitude were used for analysis. An average current was calculated from the group of IPSCs, and from this, the 10–90% rise-time could be calculated. The average IPSC was then fitted with one or a sum of exponentials to describe the decay times using the following equation:

$$y = A1 * \exp(-\frac{x}{\tau_1}) + A2 * exp\left(-\frac{x}{\tau_2}\right) + \text{residual},$$

where *A1* and *A2* are the fractions of the fast and slow components, and τ1 and τ2 are their respective decay time constants. The best fit was determined by visual inspection and by regression analysis.

A weighted decay time constant (τ_w) was also determined from the following:

$$y = \frac{\tau_1.A1 + \tau_2.A2}{(A1 + A2)}.$$

Peak scaled nonstationary noise analysis of IPSCs. Groups of IPSCs (see above) were scaled to the mean IPSC amplitude and the variance in the current decay phase was measured. The relationship between amplitude and variance was described by the following: $\delta^2 = (i.I - I^2/N_p) + \delta^2_b$, where δ^2 represents the current variance (in square picoamperes), *i* is the single channel current (in picoamperes), *I* is the mean IPSC amplitude (in picoamperes), N_p is the number of channels open at the peak of the IPSC, and δ^2_b is the baseline current variance (in square picoamperes) (Thomas et al., 2005).

Gaussian fits of IPSC distributions. IPSC data were exported from MiniAnalysis into Origin 6.0 (MicroCal Software) for analysis of the IPSC amplitude and half-width distributions. The data were fitted with

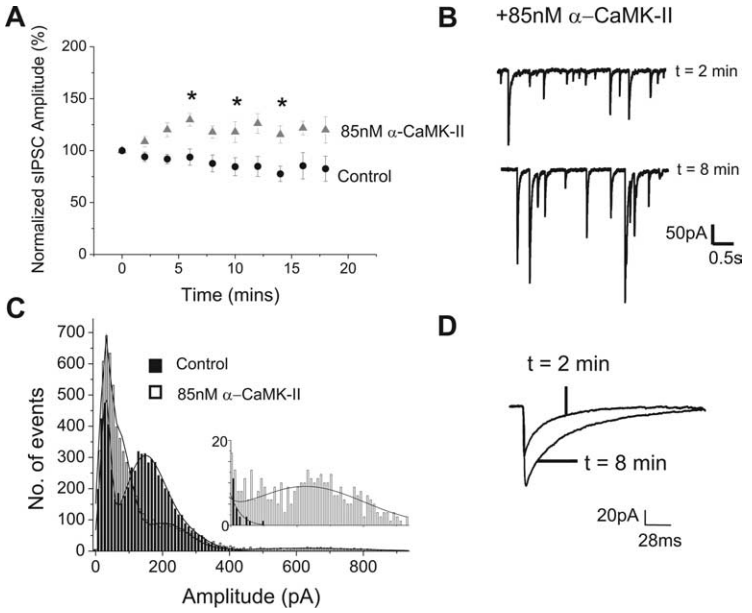

Figure 1. α-CaMK-II modulation of sIPSCs in rat CGCs in culture. ***A***, Normalized sIPSC peak amplitudes in the absence (control; $n = 9$) and presence of α-CaMK-II (85 nM; $n = 7$). In this and subsequent figures, control recordings were made using normal patch-pipette solution supplemented with preactivation buffer without α-CaMK-II. All points are mean ± SE. sIPSCs were measured in 2 min recording epochs and normalized to the mean peak amplitude obtained at $t = 0–2$ min (100%). *$p < 0.05$, *t* test. ***B***, Representative sIPSCs from a single CGC taken at $t = 2$ and 8 min using a patch-pipette solution containing α-CaMK-II. ***C***, sIPSC amplitude distributions in the absence (control; $n = 7$; 7000 events) and presence of α-CaMK-II ($n = 4$; 7000 events) obtained at $t = 6–12$ min after achieving the whole-cell configuration. The solid lines are Gaussian fits to the data. The inset shows an expanded frequency axis over the amplitude range (400–900 pA). ***D***, Averaged sIPSCs, from 50 to 100 individual events, taken from a single CGC recorded in the presence of α-CaMK-II (85 nM) at $t = 0–2$ min and at $t = 6–8$ min.

multiple Gaussian distributions (mean current, I_o; area, a_i; variance, σ) using the following function:

$$n(I) = \sum_{i=1}^{n} (a_i / \sqrt{2 \cdot \pi \cdot \sigma^2}) \cdot \exp(-(I_i - I_{0i})^2 / 2 \cdot \sigma_i^2).$$

The best fit was determined by regression analysis.

Statistics. For the statistical comparison of two means, the unpaired Student *t* test was used, unless the SDs were found to be significantly different with an *F* test, in which case the *t* test with a Welch correction was used or, alternatively, the nonparametric Mann–Whitney test was used. With groups of two or more means, one-way ANOVA was used with a Bonferroni *post hoc* test. With all statistical tests, two means were considered significantly different if $p < 0.05$. All statistical tests used GraphPad Instat version 3.01 (GraphPad).

Cluster analysis for IPSCs. To allocate IPSCs into discrete clusters for the sIPSC amplitude and half-decay times data, we used both an unsupervised hierarchical cluster analysis as well as a *k*-means cluster analysis based on Ward's method. We used *z* score normalization, and the gaps between data points were calculated using euclidian squared distances (SPSS, version 14).

Results

Cerebellar granule neurons were chosen to investigate the role of CaMK-II on inhibitory synaptic transmission because they support phosphorylation-induced modulation of native and recombinant $GABA_A$ receptors (Houston and Smart, 2006) and they also express $GABA_A$ receptors containing β2 and β3 subunits (Laurie et al., 1992; Pirker et al., 2000).

Modulation of sIPSC amplitudes by CaMK-II

We pharmacologically isolated sIPSCs in whole-cell recordings from CGCs at 7–10 DIV by bath-applying AP-5 and CNQX to block glutamate receptor activity, and incorporating QX-314 in the patch pipette solution to prevent action potentials. Virtually all IPSCs in these cultures are spontaneous and action potential-dependent and abolished by 0.5 μM TTX (Leao et al., 2000; Farrant and Brickley, 2003). Internally applying preactivated α-CaMK-II (85 nM) to CGCs via the patch pipette solution (Houston and Smart, 2006) caused a significant increase in the mean peak amplitude of sIPSCs (129.7 ± 6.1%; $n = 7$) when compared with control cells not exposed to α-CaMK-II (93.7 ± 7.8%; $n = 9$) (Fig. 1*A*,*B*,*D*). The control sIPSC amplitude histogram was best fit by the sum of three Gaussian distributions (Fig. 1*C*; supplemental Table 1, available at www.jneurosci.org as supplemental material). This increased to four Gaussian distributions in the presence of α-CaMK-II with a shift toward higher sIPSC amplitudes and the appearance of a new peak at ~600 pA (Fig. 1*C*; supplemental Table 1, available at www.jneurosci.org as supplemental material). The frequency of sIPSCs remained unaltered by α-CaMK-II (2.2 ± 0.6 Hz; $n = 7$) compared with control (2.8 ± 1.2 Hz; $n = 8$; $p > 0.05$).

Modulation of sIPSC decays by CaMK-II

The decay phase of sIPSCs, under control conditions and in the presence of α-CaMK-II, was best described by biexponentials. α-CaMK-II increased both the fast (τ_1) and slow (τ_2) decay time constants from 10 ± 0.9 to 22.7 ± 3.2 ms and from 46.7 ± 6 to 78 ± 10 ms, respectively ($n = 7–8$) (Fig. 2*A*). The proportion of the relative areas (*A1*:*A2*) for τ_1 and τ_2 were not altered by α-CaMK-II (*A1*: control, 53.6 ± 4.7%; plus α-CaMK-II, 51.7 ± 3.6%), whereas the overall weighted decay time constant (τ_w) was significantly increased from 26.1 ± 1.7 to 49.9 ± 5.7 ms (Fig. 2*B*). In contrast, α-CaMK-II did not affect the mean rise times of sIPSCs, determined between 10 and 90% of the peak sIPSC amplitude (control, 1.2 ± 0.2 ms; plus α-CaMK-II, 1.1 ± 0.1 ms; $n = 7–8$).

Variation in CaMK-II modulation of CGC sIPSCs

Previously, α-CaMK-II was demonstrated to differentially modulate β2 and β3 subunit-containing recombinant $GABA_A$ receptors (Houston and Smart, 2006). Given that CGCs express both these β subunits, it is conceivable that α-CaMK-II could have differential effects on sIPSCs. This was addressed by using a cluster analysis of scatter plots of sIPSC amplitudes against their decay half-widths ($\tau_{50\%}$), recorded in the absence (control) and presence of 85 nM α-CaMK-II.

Under control conditions, significant variation in the decay half-widths ($\tau_{50\%}$) was observed, which was not simply correlated with the sIPSC amplitudes (Fig. 2*C*). This was unlikely to be attributable to dendritic filtering because CGCs are electronically compact, but it could reflect the presence of multiple receptor subtypes with different kinetic properties. Cluster analysis revealed two main sIPSC clusters at 80.8 pA and 13 ms, and

226.4 pA and 18.1 ms. The addition of α-CaMK-II had little effect on the first cluster (63.4 pA; 14.4 ms), whereas the second cluster now reflected a population of sIPSCs with increased decay times with relatively little change in their amplitudes (241.2 pA; 29.9 ms) (Fig. 2*D*). However, α-CaMK-II also caused a subpopulation of sIPSCs to shift to much larger amplitudes with relatively little change in their decay times, which formed a new third cluster around 661.5 pA and 28.3 ms (Fig. 2*D*). Overall, these data are most simply explained by α-CaMK-II having differential effects on different populations of $GABA_A$ receptors.

α-CaMK-II modulation of sIPSCs recorded from wild-type and $\beta2^{-/-}$ mice

To discern whether the differential modulation of sIPSCs by α-CaMK-II was a consequence of its action at different $GABA_A$ receptor isoforms containing β2 or β3 subunits, we used a β2 subunit knock-out ($\beta2^{-/-}$) line (Sur et al., 2001). We discounted a role for β1 subunits because CGCs express only low levels of this subunit (Laurie et al., 1992; Pirker et al., 2000). Dissociated cerebellar cultures were prepared from $\beta2^{-/-}$ and wt mouse strains of the same genetic background (50% C57BL/6; 50% 129SvEv) (Sur et al., 2001). Although α-CaMK-II increased the mean peak sIPSC amplitude for wt CGCs from 44.9 ± 7.6 to 95.4 ± 21.3 pA (n = 9–12), it did not affect the mean sIPSC amplitude in $\beta2^{-/-}$ CGCs (control, 47.1 ± 8.1 pA; plus α-CaMK-II, 46.6 ± 5.6 pA; n = 8–9) (Fig. 3*A*,*B*; supplemental Table 2, available at www.jneurosci.org as supplemental material). In comparison, the sIPSC frequencies for wt and $\beta2^{-/-}$ were unaffected by α-CaMK-II (wt: control, 3.5 ± 0.8 Hz; plus α-CaMK-II, 2.4 ± 0.8 Hz; $\beta2^{-/-}$: control, 2.6 ± 1 Hz; plus α-CaMK-II, 2.5 ± 0.7 Hz; n = 8–12).

The amplitude distributions for wt control sIPSCs revealed three populations of synaptic currents: two with means <100 pA and the other at ~150 pA (Fig. 3*C*; supplemental Table 3, available at www.jneurosci.org as supplemental material). The sIPSC distribution after α-CaMK-II required four Gaussians, including an emerging population with a mean of ~30 pA and large variance, increasing the number of events in the range 50–100 pA. In addition, the largest amplitude sIPSC population was displaced to the right by α-CaMK-II (Fig. 3*D*).

In comparison, the amplitude distribution for control sIPSCs recorded from $\beta2^{-/-}$ cultures was similar to that for wt cells with three Gaussian populations, two of which are <100 pA and another between 100 and 300 pA (Fig. 3*D*; supplemental Table 3, available at www.jneurosci.org as supplemental material). After exposure to α-CaMK-II, a fourth Gaussian again appeared with a large variance; however, in contrast to the wt CGCs, there was no increase in the amplitude of the largest sIPSC population. This

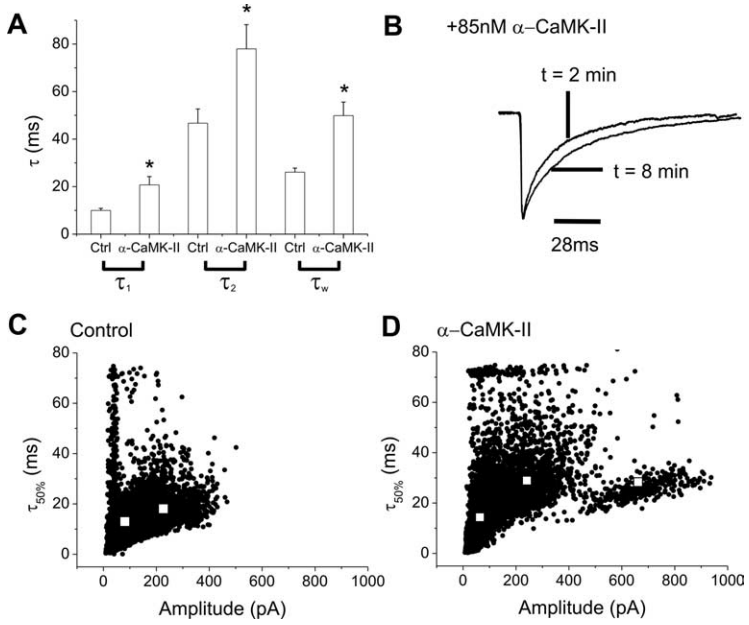

Figure 2. α-CaMK-II modulation of sIPSC decay times in rat CGCs in culture. ***A***, Bar chart of the mean decay time constants, τ_1 and τ_2, and the weighted decay time, τ_w, at t = 6–12 min in the absence (control; n = 8) and presence of α-CaMK-II (n = 7). *$p < 0.05$, t test to compare controls with α-CaMK-II. Error bars indicate SE. ***B***, Representative averaged sIPSCs from 50 to 100 individual sIPSCs from a single CGC recorded in the presence of α-CaMK-II (85 nM) at t = 0–2 min and at t = 6–8 min. sIPSCs are rescaled to the same amplitude. ***C***, ***D***, Scatter plots of sIPSC amplitudes and decay half-widths ($\tau_{50\%}$) at t = 6–12 min in the absence (***C***) (control; n = 7; 7000 events) and presence (***D***) of α-CaMK-II (85 nM; n = 4; 7000 events). Coordinates defined by cluster analyses are shown as white squares.

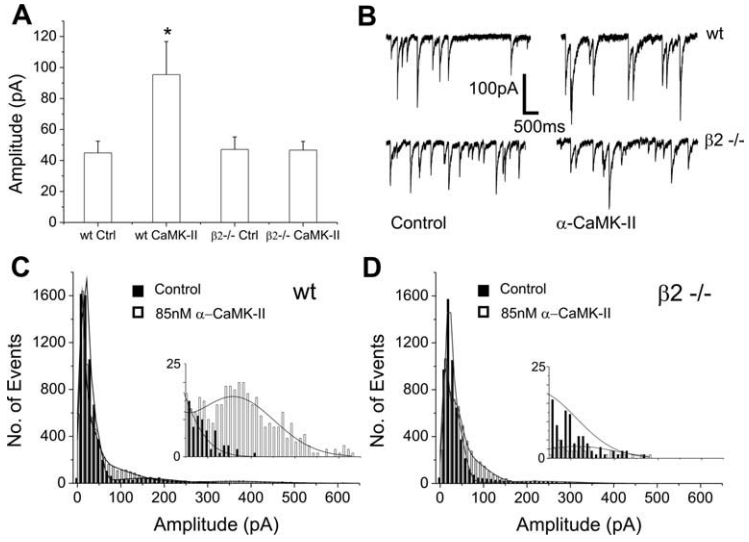

Figure 3. α-CaMK-II modulation of sIPSCs from wt and $\beta2^{-/-}$ mouse CGCs. ***A***, Bar chart showing the mean peak sIPSC amplitudes in the absence and presence of α-CaMK-II (85 nM) recorded from wt (control, n = 9; plus α-CaMK-II, n = 12) and $\beta2^{-/-}$ (control, n = 8; plus α-CaMK-II, n = 9) CGC cultures (t = 6–12 min). *$p < 0.05$, ANOVA with a Bonferroni posttest to compare controls with α-CaMK-II groups. Error bars indicate SE. ***B***, Representative sIPSCs recorded from single wt and $\beta2^{-/-}$ CGCs in the absence and presence of α-CaMK-II. ***C***, Amplitude distribution histogram of sIPSCs in the absence (control; n = 8; 6300 events) and presence (n = 11; 6300 events) of α-CaMK-II recorded from wt mouse cultures. The inset shows an expanded frequency over the amplitude range 250–650 pA. ***D***, sIPSC amplitude distributions in the absence (control; n = 9; 5500 events) and presence (n = 10; 5500 events) of α-CaMK-II for $\beta2^{-/-}$ CGCs. The inset expands the frequency of IPSCs over the range 250–650 pA.

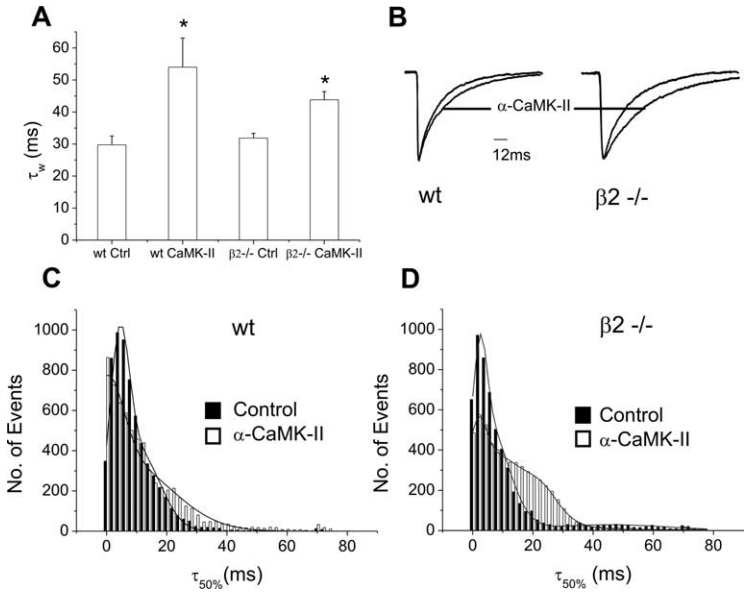

Figure 4. α-CaMK-II modulation of sIPSC decays in wt and $\beta2^{-/-}$ CGCs. ***A***, Bar chart of the mean weighted decay time constants (τ_w) in the absence (control; $n = 7$) and presence ($n = 7$) of α-CaMK-II for sIPSCs recorded from wt and $\beta2^{-/-}$ (control, $n = 6$; α-CaMK, $n = 6$) CGCs. *$p < 0.05$, ANOVA with a Bonferroni posttest to compare controls with α-CaMK-II groups. Error bars indicate SE. ***B***, Representative average sIPSCs from 50 to 100 individual currents recorded from single wt and $\beta2^{-/-}$ CGCs in the absence and presence of α-CaMK-II. sIPSCs are rescaled to the same amplitude. ***C***, ***D***, Half-width ($\tau_{50\%}$) distributions for sIPSCs in the absence and presence of α-CaMK-II recorded from wt (***C***) (control, $n = 8$, 6300 events; plus α-CaMK-II, $n = 11$, 6300 events) and $\beta2^{-/-}$ CGCs (***D***) (control, $n = 9$, 5500 events; plus α-CaMK-II, $n = 10$, 5500 events).

suggests that the β2 subunit is important for the upregulation of the largest amplitude population of sIPSCs. Despite the increase in the number of sIPSCs around 50–100 pA range in $\beta2^{-/-}$ cultures, this change was insufficient to alter the mean peak IPSC amplitude.

CaMK-II modulation of decay times in $\beta2^{-/-}$ mice

The decay times for averaged sIPSCs continued to be described by a biexponential. Ablating the β2 subunit altered neither the mean decay times (τ_1; τ_2) for IPSCs nor their relative areas under control conditions (supplemental Table 2, available at www.jneurosci.org as supplemental material).

Application of α-CaMK-II significantly increased the weighted decay times (τ_w) and both τ_1 and τ_2 for sIPSCs recorded either from wt or $\beta2^{-/-}$ cultures (Fig. 4*A*,*B*; supplemental Table 2, available at www.jneurosci.org as supplemental material). The relative area for τ_1 was not significantly different in the presence of α-CaMK-II for wt (CaMK-II, 64.4 ± 3.6%; control, 56.3 ± 5.5%; $n = 7$) or $\beta2^{-/-}$ cultures (CaMK-II, 61.3 ± 2.7%; control, 53.1 ± 5.8%; $n = 6$). The mean rise times of averaged sIPSCs were also unaltered between wt (α-CaMK-II, 1.39 ± 0.15 ms; control, 1.15 ± 0.15 ms; $n = 7$) or $\beta2^{-/-}$ cultures (α-CaMK-II, 1.45 ± 0.18 ms; control, 0.98 ± 0.16 ms; $p > 0.05$). Therefore, removing the β2 subunit had little effect on the lengthening of the sIPSC decays by α-CaMK-II, and thus a different β subunit must underpin this kinetic effect.

To fit the distribution of all sIPSC half-widths ($\tau_{50\%}$) for wt cultures required two Gaussians. The application of CaMK-II increased the relative proportion of the slower half-width population at the expense of the fastest (Fig. 4*C*). For $\beta2^{-/-}$ CGCs, the distribution of sIPSC half-widths in control conditions is similar to that for wt cultures, but with the addition of a third population of slower-decaying events. The low frequency of these events was insufficient to alter the mean τ_w. After exposure to α-CaMK-II, sIPSCs from $\beta2^{-/-}$ cultures also displayed an increase in half-width, but now, four Gaussians were necessary to fit the distribution, because of an additional population of slower-decaying events of ~24 ms (Fig. 4*D*; supplemental Table 4, available at www.jneurosci.org as supplemental material). The small proportion of larger half-width sIPSCs seen in controls is still present and appears relatively unchanged.

Variation in CaMK-II modulation of wt and $\beta2^{-/-}$ CGC sIPSCs

To determine whether particular $GABA_A$ receptors could be associated with populations of sIPSCs in wt and $\beta2^{-/-}$ neurons, scatter plots of sIPSC half-width against amplitude were constructed. For sIPSCs recorded from wt cultures under control conditions, two clusters of synaptic events were identified (Fig. 5*A*). One cluster at 32.6 pA and 9.3 ms represented sIPSCs with amplitudes <100 pA that are associated with a broad range of decay times. The second (218.4 pA; 20.3 ms) signified a distinct population of sIPSCs of 100–300 pA amplitude with much less variation in the half-width of 10–30 ms. Scatter plots of sIPSCs from $\beta2^{-/-}$ cultures under control conditions were also described by two clusters (35.6 pA, 9 ms; 217.9 pA, 50.3 ms) (Fig. 5*C*) revealing that the largest amplitude population displayed variable half-widths mostly over 30 ms, accounting for the small number of very slow-decaying synaptic events observed in $\beta2^{-/-}$ cultures. This change in half-width implied that the larger-amplitude events seen in the wt cultures are most likely supported by β2 subunit-containing $GABA_A$ receptors.

After applying α-CaMK-II to wt cultures, both sIPSC half-widths and amplitudes appeared to increase (Fig. 5*B*). The first cluster was relatively unaltered (28.3 pA; 10.3 ms) but the largest amplitude sIPSCs of 100–300 pA were now split into two clusters to accommodate a new population of even higher-amplitude sIPSCs (135.8 pA, 23.7 ms; 388.1 pA, 23.1 ms) (Fig. 5*B*).

Three clusters were also identified after applying α-CaMK-II to $\beta2^{-/-}$ cultures (Fig. 5*D*). The first cluster is relatively unaltered from control (35.5 pA; 12 ms), whereas a new cluster of sIPSCs appeared at 97.5 pA and 23.5 ms, most likely associated with β3 subunit-containing receptors (Fig. 5*D*). However, the cluster of large-amplitude sIPSCs >300 pA remained relatively unaltered when compared with $\beta2^{-/-}$ controls (310.2 pA; 43.2 ms). These findings suggest that the loss of α-CaMK-II regulation on β2 subunit-containing receptors prevented the increase in sIPSC amplitude.

Peak-scaled nonstationary noise analysis

To understand how CaMK-II was increasing sIPSC amplitudes by modulating different populations of $GABA_A$ receptors, we used peak-scaled nonstationary noise analysis of sIPSCs recorded from wt mouse CGCs, which were grouped according to the cluster analysis. Essentially, sIPSCs were allocated into small- or large-amplitude clusters depending on whether their amplitudes were smaller or larger than 150 pA. This grouping was also

thought to split $\beta 2$ subunit-mediated sIPSCs (>150 pA) from those likely to be mediated by $\beta 3$ subunit-containing receptors (<150 pA) because this latter population was relatively unchanged in the $\beta 2^{-/-}$ mouse. For the two clusters of sIPSCs, unitary current (*i*) was unaffected by α-CaMK-II (Fig. 6*A*). However, the average number of active channels open at the peak of the IPSC (N_p) was significantly increased by α-CaMK-II in the >150 pA ($\beta 2$) group from 114 ± 8 to 151 ± 11 ($n = 4$), whereas in the <150 pA ($\beta 3$) group, there was no significant change (control, 30 ± 8, $n = 4$; α-CaMK-II, 44 ± 16, $n = 6$) (Fig. 6*B*). This differential effect of α-CaMK-II on the number of active channels for only the >150 pA ($\beta 2$) cluster suggests the mechanism of action for α-CaMK-II was specific to discrete $GABA_A$ receptor isoforms.

To determine the relative charge transfers for $\beta 2$ and $\beta 3$ subunit-containing synaptic receptor populations, we regrouped the sIPSCs recorded from the wt mouse into >150 and <150 pA and normalized the mean charge transfer (in picocoulombs) to cell capacitance (in picofarads). For the <150 pA ($\beta 3$) sIPSC group, the mean charge transfer increased from 49.9 ± 12.9 pC/pF ($n = 8$; control) to 191 ± 85.5 pC/pF on addition of α-CaMK-II ($n = 9$; $p < 0.05$). For the >150 pA ($\beta 2$) sIPSCs, the mean charge transfer also increased from 283.4 ± 95.2 pC/pF ($n = 8$; control) to 836.6 ± 170 pC/pF ($n = 9$; $p < 0.05$) in the presence of α-CaMK-II. The proportion of total charge transfer mediated by each receptor population under control conditions was <150 pA ($\beta 3$), 68 ± 11%, and for >150 pA ($\beta 2$), 32 ± 11%. After α-CaMK-II, the proportions were unaltered (<150 pA ($\beta 3$), 58 ± 11%; >150 pA ($\beta 2$), 42 ± 11%; $p > 0.05$). This indicated that, although CaMK-II increased the charge transfer mediated by $\beta 2$ and $\beta 3$ synaptic receptors via different mechanisms, the relative weight of charge movement between $\beta 2$ and $\beta 3$ receptors remains the same.

To confirm that $\beta 3$ subunits were the predominant remaining β subunit in the $\beta 2^{-/-}$ mouse cultures, we applied the $\beta 1$ subunit-selective inhibitor, salicylidene salicylhydrazide (SCS) (Thompson et al., 2004). The mean amplitude and the frequency of sIPSCs were unaffected by 1 μM SCS when compared with control measurements (=100%) taken before SCS application (amplitude, 91 ± 9%; frequency, 82 ± 12%; $n = 5$). This indicated that the $\beta 1$ subunit was either not present or expressed at a very low level in CGCs.

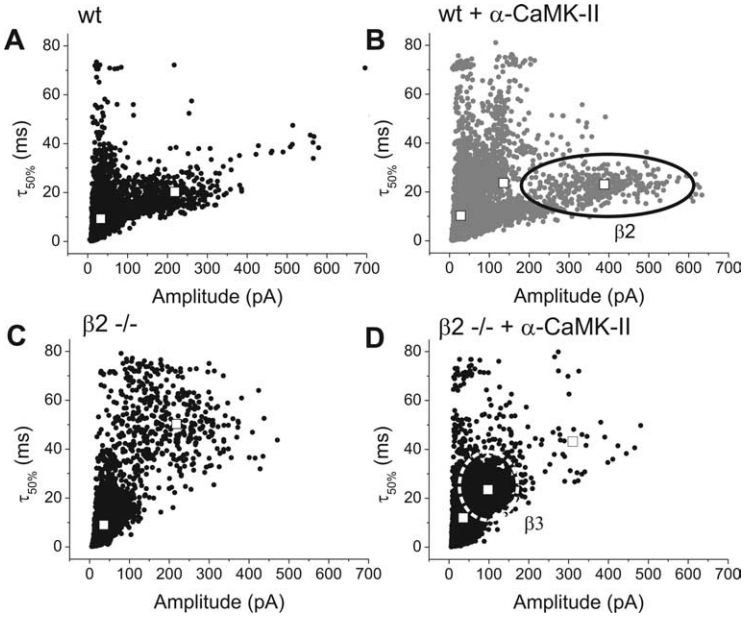

Figure 5. Scatter plots of sIPSC amplitude and decay half-width for wt and $\beta 2^{-/-}$ CGCs. ***A–D***, Scatter plot of sIPSC amplitudes and half-widths ($\tau_{50\%}$) in the absence (***A***) (control; $n = 8$; 6300 events) and presence of 85 nM α-CaMK-II (***B***) ($n = 11$; 6300 events) recorded from wt mouse cultures. Similar scatter plots in the absence (***C***) (control; $n = 9$; 5500 events) and presence (***D***) ($n = 9$; 5500 events) of α-CaMK-II recorded from $\beta 2^{-/-}$ CGCs. sIPSCs potentially mediated by $\beta 2$ subunit-containing receptors are indicated by the solid line. The dashed line indicates sIPSCs potentially mediated by predominantly $\beta 3$ subunit-containing receptors. Cluster coordinates are overlaid (white squares).

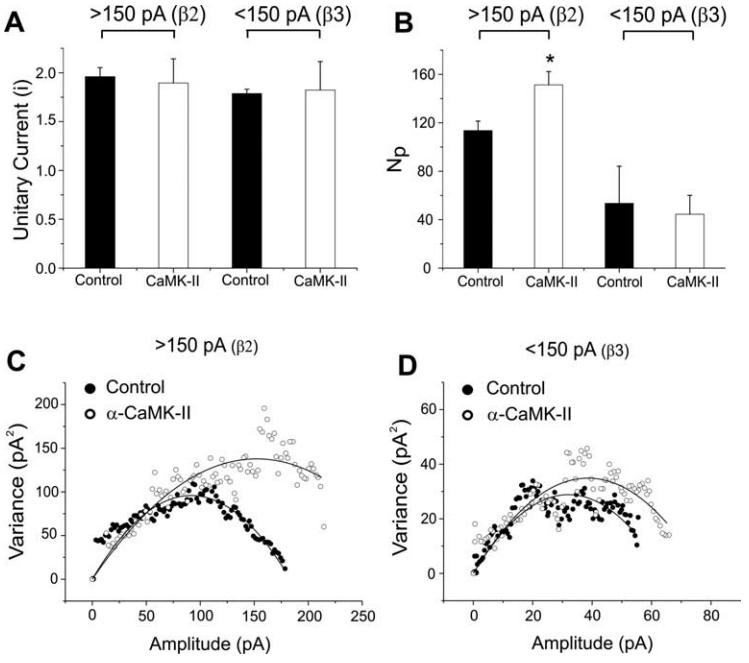

Figure 6. Peak-scaled nonstationary noise analysis of sIPSCs from wt CGCs. ***A***, ***B***, Bar charts showing the single channel current (*i*) (***A***) and the average number of active channels (N_p) (***B***) in the absence and presence of α-CaMK-II (85 nM) for sIPSCs with amplitudes <150 pA and >150 pA ($n = 4–6$). *$p < 0.05$ for α-CaMK-II compared with control using ANOVA (Bonferroni's posttest). Error bars indicate SE. ***C***, ***D***, Synaptic current–variance relationships from single cells in the absence and presence of α-CaMK-II for sIPSCs >150 pA (***C***) and <150 pA (***D***) in amplitude.

Immunocytochemistry

The electrophysiological data suggested that $\beta 2$ and $\beta 3$ subunit-containing receptors are localized to two distinct populations of inhibitory synapses. To corroborate this, we used $\beta 2$ and $\beta 3$ subunit-specific antibodies to immunocytochemically label in-

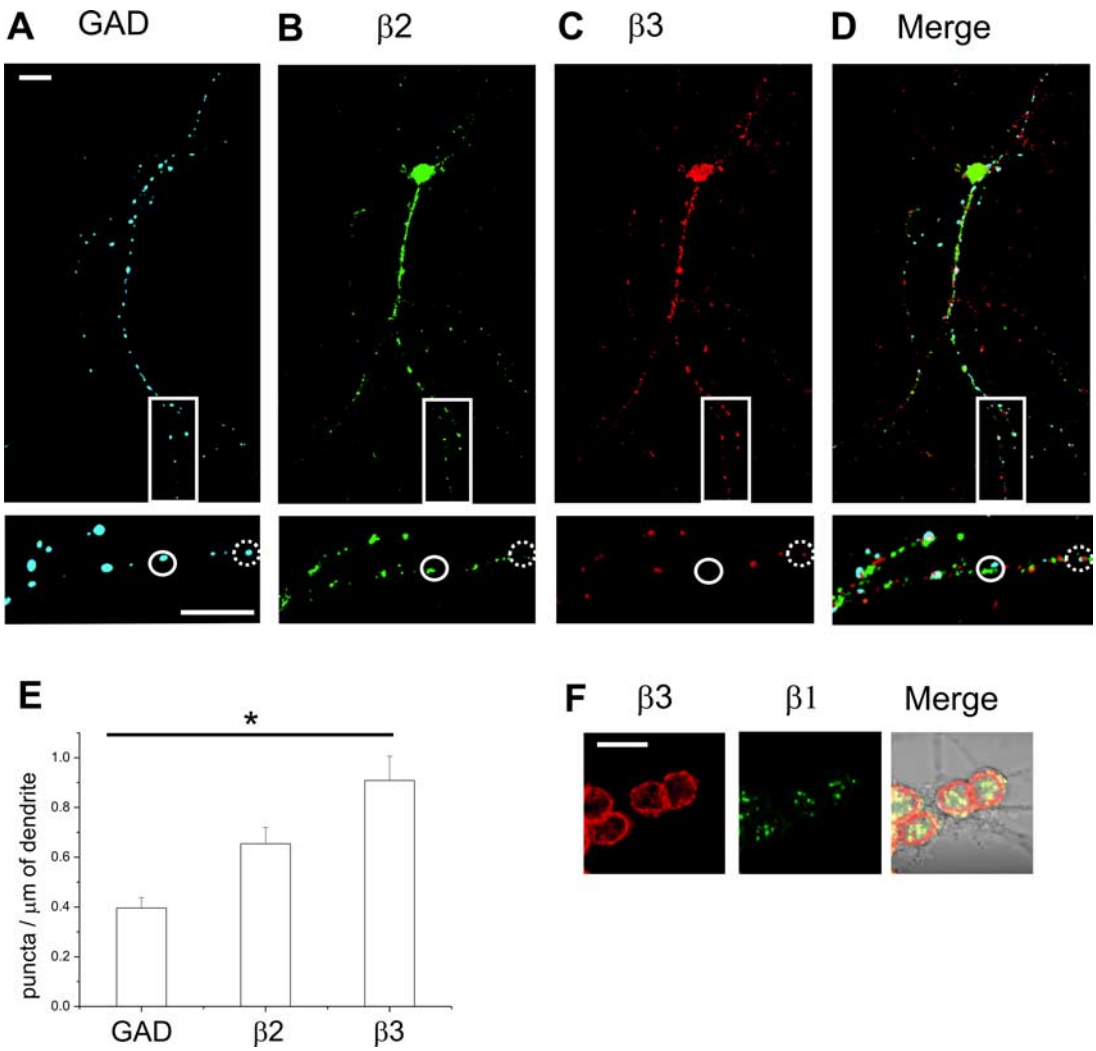

Figure 7. Immunocytochemistry of β1–3 subunits. ***A–D***, Image of a CGC immunolabeled with anti-GAD (***A***) (Cy5) to label inhibitory presynaptic terminals; anti-β2 subunit antibodies (***B***) (Cy2) and anti-β3 subunit (rabbit anti-β3) (***C***) (Rhodamine Red-X), with an overlay of all three panels (***D***). The insets show expanded regions of dendrites to resolve individual puncta. The circles identify β2 (solid) or β3 (dashed) subunit puncta located in apposition to GAD puncta. ***E***, Summary bar chart of the mean densities (number of puncta/micrometer length of dendrite; $n = 9$). *$p < 0.05$, ANOVA. Error bars indicate SE. ***F***, Image of $\beta2^{-/-}$ CGCs immunolabeled with anti-β3 subunit (goat anti-β3) and anti-β1 subunit antibodies, with an overlay on a differential interference contrast brightfield image. Scale bar, 10 μm.

hibitory synapses in cultured CGCs, together with an antibody against GAD to identify inhibitory presynaptic terminals. The relative densities of immunofluorescent puncta were assessed to determine the distribution of individual $GABA_A$ receptor subunits.

Inhibitory synapses, as defined by the presence of GAD puncta, were present at a density of $0.39 \pm 0.03/\mu$m of dendrite (Fig. 7*A*,*E*). Puncta containing β3 subunits were observed at a higher density of $0.94 \pm 0.09/\mu$m of dendrite, whereas β2 puncta occurred less frequently at $0.68 \pm 0.08/\mu$m of dendrite (Fig. 7*B*,*C*,*E*) ($n = 9$). The higher density of β2 and β3 subunit puncta, compared with GAD, suggested a number of β2 and β3 puncta resided at extrasynaptic locations (Fig. 7*D*). Typically, β2 and β3 subunit puncta were often noted to be independent of one another, supporting the view that they are frequently localized to different inhibitory synapses. Identical results were obtained using a β3 antibody raised in a different species (see Materials and Methods) (supplemental Fig. 1*A–D*, available at www.jneurosci.org as supplemental material).

By comparing immunofluorescence for β1 and β3 subunits in wt and $\beta2^{-/-}$ cultures, it was evident that β1 labeling was never found on cell surface membranes in the dendrites (Fig. 7*F*). However, some β1 labeling was observed in the cell soma, but mostly located to intracellular compartments. This contrasted with the strong β3 subunit staining on somatic and dendritic surface membranes, indicating that the β3 subunit is indeed the primary subunit that is expressed in $\beta2^{-/-}$ cultures.

Importance of Ca^{2+}/CaM binding to CaMK-II

Comparing different forms of α-CaMK-II in transfected neurons on synaptic $GABA_A$ receptors indicated that mutant forms of α-CaMK-II that are constitutively active and Ca^{2+}-independent (T286D) or capable of only transient Ca^{2+}-dependent activation (T286A) significantly increased the peak amplitude of IPSCs without changing decay kinetics (EGFP control, 147.6 ± 22.5 pA; T286D, 241.7 ± 33 pA; T286A, 263.5 ± 41 pA) (Fig. 8*A*,*D–F*). However, mutated α-CaMK-II that either blocked Ca^{2+}/CaM binding (A302R) or inhibited kinase activity (K42R) (Shen and Meyer, 1999) reduced sIPSC amplitudes (A302R, 87.2 ± 12.4 pA; K42R, 64.4 ± 11.5 pA) (Fig. 8*A*,*D*,*G*,*H*) and decay times (GFP,

32.8 ± 3.1 ms; A302R, 25.2 ± 1.6 ms; K42R, 23.7 ± 1.2 ms) (Fig. 8*B*,*C*).

These variations in sIPSC amplitudes were not a consequence of cell size because the mean cell capacitances were not significantly different for any of the transfected cells (GFP, 7.1 ± 1.2 pF; T286D, 7.5 ± 0.92 pF; T286A, 8.5 ± 0.5 pF; A302R, 7.6 ± 0.6 pF; K42R, 8.4 ± 0.8 pF). Moreover, the actions of α-CaMK-II were purely postsynaptic because α-CaMK-II mutants did not affect sIPSC frequency (GFP, 3.8 ± 1 Hz; T286D, 2.1 ± 0.3 Hz; T286A, 3.3 ± 0.7 Hz; A302R, 4.7 ± 0.8 Hz; K42R, 3.3 ± 1.1). Thus, Ca^{2+}/CaM binding, rather than autophosphorylation of Thr^{286}, was critically required for α-CaMK-II modulation of synaptic $GABA_A$ receptors. These data also suggest a role for endogenous CaMK-II in CGCs to enhance the amplitude and prolong the decay of sIPSCs leading to increased charge transfer across the inhibitory synapse.

This was investigated by recording from rat cultured granule cells by delivering the CaMK-II inhibitor, CaMK-II-Ntide (Chang et al., 1998), via the patch pipette. The sIPSC amplitudes and decay times were measured 12–14 min after the start of the whole-cell recording and normalized to mean values determined within the first 3–5 min. The sIPSC amplitude was not significantly affected by CaMK-II-Ntide (95.8 ± 5.3%; $n = 8$) compared with control (97.8 ± 4%, $n = 6$), but the decay times were reduced with respect to a scrambled peptide control (CaMK-II-Ntide, 96.4 ± 4%, $n = 8$; control, 111 ± 4.7%, $n = 6$). Thus, basal activity of CaMK-II slightly affects only the decay times of sIPSCs and presumably β3-containing synaptic receptors.

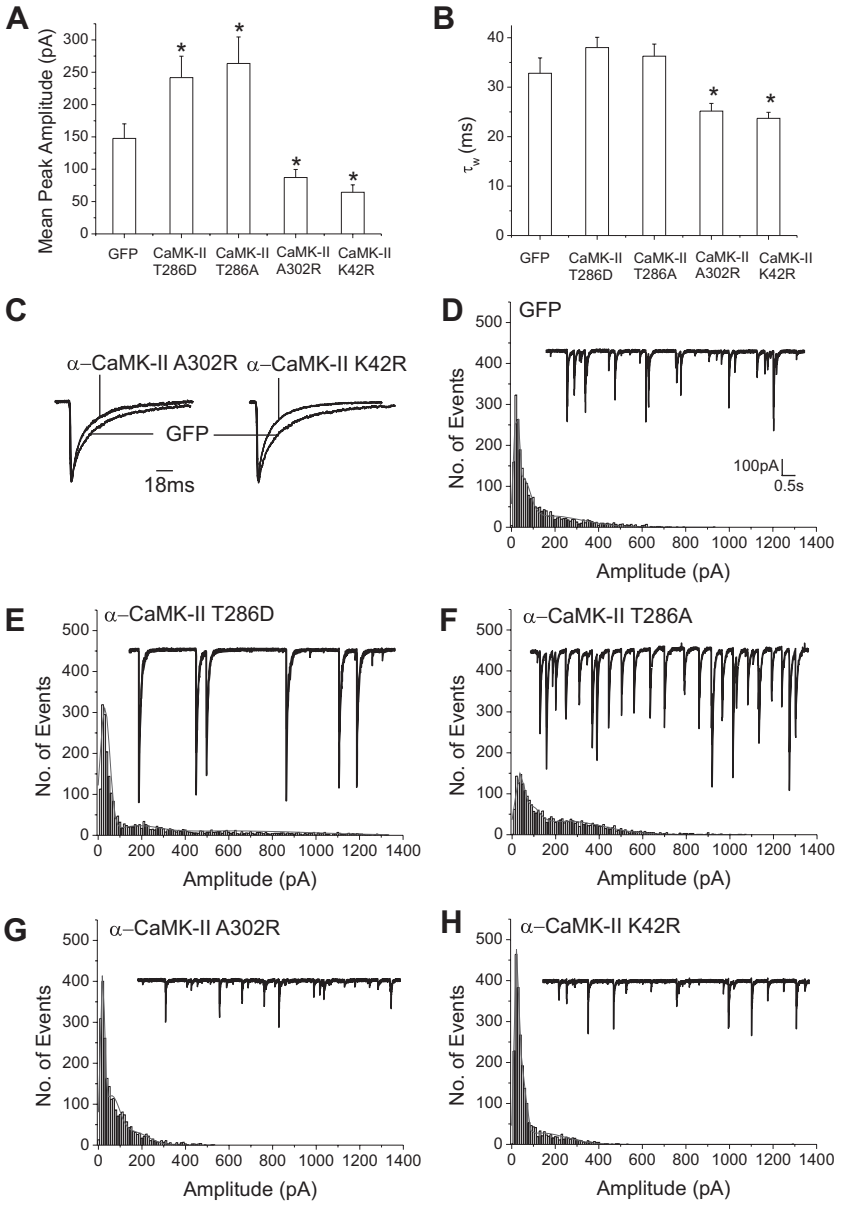

Figure 8. sIPSCs and mutant α-CaMK-II in CGCs. ***A***, ***B***, Bar chart of the mean peak sIPSC amplitude (***A***) and weighted decay time constant (τ_w) (***B***) obtained from CGCs expressing α-CaMK-II T286D; T286A; A302R; K42R; or just GFP as a control ($n = 6–8$). $^*p < 0.05$, using ANOVA with a Bonferroni posttest to compare α-CaMK-II mutants to the GFP-only control. Error bars indicate SE. ***C***, Scaled average sIPSCs (50–100 IPSCs) from single CGCs expressing GFP only, α-CaMK-II A302R, or α-CaMK-II K42R. ***D–H***, sIPSC amplitude histograms were taken from rat CGCs expressing GFP (2380 events; $n = 6$) (***D***); α-CaMK-II T286D (2380 events; $n = 4$) (***E***); α-CaMK-II T286A (2250 events; $n = 4$) (***F***); α-CaMK-II A302R (2390 events; $n = 6$) (***G***); α-CaMK-II K42R (2390 events; $n = 6$) (***H***). The insets show representative sIPSCs. The calibration in ***D*** applies also to ***E–H***.

Discussion

It is currently unclear whether phosphorylation can differentially affect the function of synaptic receptors expressing different β subunits at individual inhibitory synapses. Here, we show, using a combination of electrophysiology, imaging, and transgenic mice, that the acute application of α-CaMK-II can increase the amplitude and decay times of sIPSCs recorded from rat and mouse cerebellar granule cells in culture. By using a β2 $GABA_A$ receptor subunit knock-out mouse, we revealed that α-CaMK-II phosphorylation has a different functional effect on β2 compared with β3 subunit-containing receptors at inhibitory synapses. It appeared that α-CaMK-II acted on β2 subunit-containing receptors to increase the peak amplitude without affecting decay kinetics, whereas on β3 subunit-containing receptors, α-CaMK-II mostly prolonged the sIPSC decay.

Distinct synapses express $GABA_A$ receptors containing β2 or β3 subunits

By comparing populations of sIPSCs recorded from wt and $\beta2^{-/-}$ CGCs, we attributed the large-amplitude fast-decaying sIPSCs, whose amplitudes, but not decays, were modulated by α-CaMK-II, to β2 subunit-containing $GABA_A$ receptors. Although compensatory changes to the expression levels of other β subunits might occur after removing the β2 subunit (Ponomarev et al., 2006), it seems unlikely that β1 subunit expression is increased because its expression is at best minimal in CGCs (Laurie et al., 1992; Pirker et al., 2000), which we confirmed in our $\beta2^{-/-}$ CGCs by the ineffectiveness of SCS and by immunocytochemistry. Thus, in CGCs, synaptic β2 subunit-containing receptors

appear to be modulated by α-CaMK-II. This contrasts with the lack of modulation by α-CaMK-II of recombinant α1β2γ2S receptors expressed in NG108-15 cells (Houston and Smart, 2006), which implies that the neuronal inhibitory synaptic environment is vitally important for supporting α-CaMK-II modulation of $GABA_A$ receptor isoforms. We also concluded that $GABA_A$ receptors containing β3 subunits mediated the smaller-amplitude, variable-decay sIPSCs whose decay rates are prolonged by α-CaMK-II. Thus, the functional effect and therefore the mechanism of α-CaMK-II modulation differed between β2 and β3 subunit-containing synaptic $GABA_A$ receptors. Additional support for our hypothesis that β2 and β3 subunits may form distinct synapses was obtained from immunocytochemistry in which we were able to detect differential localization of β2 and β3 subunits.

Differential regulation of receptor function by α-CaMK-II accords with β2 and β3 subunits binding differentially to kinase anchoring and also trafficking proteins. For example, AKAP 79/150 binds to β1 and β3 subunits, but not to β2, which facilitates their phosphorylation by PKA (protein kinase A) (Brandon et al., 2003). In contrast, a $GABA_A$ receptor-associated protein, GRIF-1, a potential trafficking factor, binds to β2 and not β1 or β3 subunits (Beck et al., 2002). Additional evidence suggests that the trafficking and targeting of β2 and β3 subunit-containing receptors to the cell surface is also different (Connolly et al., 1996) and that these processes can be differentially affected by phosphorylation (Ives et al., 2002). Thus, the functional consequences of phosphorylation of different β subunits could depend on their distinctive association with proteins in the postsynaptic density.

Mechanism of action

The distinctive functional effects of α-CaMK-II on synaptic $GABA_A$ receptors suggested that different mechanisms are involved in the regulation of β2 compared with β3 subunit-containing receptors. Nonstationary noise analysis suggested that α-CaMK-II increased N_p for sIPSCs >150 pA (proposed β2 subunit-mediated) compared with sIPSCs <150 pA (proposed β3 subunit-mediated), in which there was no effect. The increased N_p for the β2 subunit-containing group suggested that either new receptors were inserted into the membrane and/or the channel open probability had increased. An increase in the number of cell surface receptors through insertion or altered membrane trafficking would be consistent with an increase in IPSC amplitude without altering decay. Interestingly, protein kinase B can increase the number of cell surface $GABA_A$ receptors by phosphorylating Ser^{410} in the β2 subunit, resulting in an increase in mIPSC amplitude without affecting decay (Wang et al., 2003).

An increase in channel open probability could potentially affect the decay phase of sIPSCs and also increase sIPSC amplitudes. However, an effect on amplitude would only be clearly manifest if GABA concentrations were nonsaturating at inhibitory synapses (Nusser et al., 1998). Indeed, the functional consequences of receptor phosphorylation by CaMK-II will depend, in part, on $GABA_A$ receptor occupancy, which is known to vary between cell types and even between synapses on the same cell (Nusser et al., 1997; Hájos et al., 2000).

Changes to single-channel properties, which could potentially alter decay times, may result from direct phosphorylation of the $GABA_A$ receptor. Tyrosine kinases can directly phosphorylate the γ2 subunit, and this increases mean open time and the open probability of the $GABA_A$ receptor (Moss et al., 1995). α-CaMK-II can directly phosphorylate the $GABA_A$ receptor β3 subunit and may also execute some of its effects on $GABA_A$ receptors through activation of a tyrosine kinase and phosphorylation of γ2 subunits (Houston et al., 2007).

Another possibility is that phosphorylation may affect receptor desensitization, which has been proposed to modulate IPSC decay times (Jones and Westbrook, 1996, 1997). The biexponential decay of most IPSCs is thought to reflect the $GABA_A$ receptor entering into desensitized states and the relative contribution of each phase has been shown to be modulated by phosphorylation (Nusser et al., 1999; Poisbeau et al., 1999). However, on application of α-CaMK-II to rat and mouse CGCs, there was no alteration in the relative areas of τ_1 and τ_2, which argues against such a mechanism being involved in the current study.

It is also possible that a variation in the decay rate can result from the activation of perisynaptic receptors, activated by the spillover of GABA from inhibitory synapses (Wei et al., 2003). This has been observed at cerebellar Golgi cell–granule cell synapses (Rossi and Hamann, 1998; Hamann et al., 2002). A preferential upregulation of perisynaptic $GABA_A$ receptors by α-CaMK-II-dependent phosphorylation would then be predicted to prolong the decay of IPSCs and also IPSC rise times, but this was not observed.

Significance of Ca^{2+}/CaM binding and autophosphorylation

Although a Ca^{2+}-independent, constitutively active form of CaMK-II (T286D) increased sIPSC amplitudes, the autophosphorylation-deficient (Ca^{2+}-dependent) α-CaMK-II (T286A) acted similarly. This was surprising because autophosphorylation at Thr^{286} is considered to be vital for many aspects of α-CaMK-II function (Lisman et al., 2002). Crucially, however, the T286A mutant is still capable of binding Ca^{2+}/CaM, transient activation, and translocation (Shen and Meyer, 1999; Shen et al., 2000). In contrast, the inactive α-CaMK-II mutants, A302R and K42R, reduced sIPSC decay times and amplitudes, suggesting that Ca^{2+}/CaM binding and kinase activity is critically important for α-CaMK-II modulation of $GABA_A$ receptors and that endogenous CaMK-II promotes charge transfer at inhibitory synapses. Intracellular dialysis with a peptide inhibitor that blocks Ca^{2+}-dependent and independent CaMK-II activity only slightly reduced sIPSC decay times, without any effect on sIPSC amplitudes. This disparity may be attributable to the acute application of CaMK-II-Ntide blocking only basal CaMK-II activity in neurons after inhibitory synapses are established compared with the expression of mutant α-CaMK-II in neurons before synaptogenesis (5 DIV), which could act as a dominant negative disrupting CaMK-II activity (stimulated by Ca^{2+} entry when GABA is depolarizing) to reduce sIPSC decays and amplitudes. The reduction in sIPSC decay by CaMK-II-Ntide suggests that there is a low level of basal CaMK-II activity at 7–10 DIV that acts on presumably β3 subunit-containing receptors to maintain increased decay times, whereas there is no effect on sIPSC amplitudes (β2 subunit-containing receptors). This suggests that persistent CaMK-II activity is not required to maintain sIPSC amplitudes, consistent with the observation that autophosphorylation (Thr^{286}) and Ca^{2+}-independent activity are also not required for CaMK-II to increase the amplitude of sIPSCs.

Physiological significance

Modulation of $GABA_A$ receptors by α-CaMK-II is an important mechanism for regulating the efficacy of synaptic inhibition by affecting either IPSC amplitude and/or decay times. Such a mechanism could underlie the activity-dependent formation of inhibitory synapses during development (Ben-Ari et al., 2007), as well as modulate $GABA_A$ receptors that underpin homeostatic

forms of inhibitory synaptic plasticity, such as rebound potentiation, in which strong excitatory activity causes long-term upregulation of inhibitory synaptic transmission (Kano et al., 1996; Kawaguchi and Hirano, 2002).

Dysfunction to CaMK-II signaling is implicated in several neurological disorders affecting inhibitory transmission. For example, the neurodevelopmental disorder, Angelman's syndrome, has been linked to low expression of the $GABA_A$ receptor $\beta 3$ subunit and to disrupted α-CaMK-II signaling (DeLorey et al., 1998; Weeber et al., 2003). Dysfunctional α-CaMK-II signaling is also linked to epilepsy through a proposed interaction with $GABA_A$ receptors (Churn et al., 2000; Singleton et al., 2005).

It is becoming increasingly clear that different $GABA_A$ receptor subtypes are targeted to specific locations within neurons in which they undertake different roles (Nyíri et al., 2001; Brünig et al., 2002; Herd et al., 2008). Certainly, different roles have been ascribed to $\beta 2$ and $\beta 3$ subunit-containing $GABA_A$ receptors (Rudolph and Möhler, 2004). The correlation of specific populations of sIPSCs in CGCs with $GABA_A$ receptor isoforms containing different β subunits enables phosphorylation by CaMK-II to exert a fine control over the efficacy of inhibitory transmission at specific GABAergic synapses. This type of signaling may well be a generic feature of neurotransmission at other inhibitory synapses (Huntsman and Huguenard, 2006; Ing and Poulter, 2007).

References

Beck M, Brickley K, Wilkinson HL, Sharma S, Smith M, Chazot PL, Pollard S, Stephenson FA (2002) Identification, molecular cloning, and characterization of a novel $GABA_A$ receptor-associated protein, GRIF-1. J Biol Chem 277:30079–30090.

Ben-Ari Y, Gaiarsa JL, Tyzio R, Khazipov R (2007) GABA: a pioneer transmitter that excites immature neurons and generates primitive oscillations. Physiol Rev 87:1215–1284.

Brandon N, Jovanovic J, Moss S (2002) Multiple roles of protein kinases in the modulation of γ-aminobutyric $acid_A$ receptor function and cell surface expression. Pharmacol Ther 94:113–122.

Brandon NJ, Jovanovic JN, Colledge M, Kittler JT, Brandon JM, Scott JD, Moss SJ (2003) A-kinase anchoring protein 79/150 facilitates the phosphorylation of $GABA_A$ receptors by cAMP-dependent protein kinase via selective interaction with receptor beta subunits. Mol Cell Neurosci 22:87–97.

Brünig I, Scotti E, Sidler C, Fritschy J-M (2002) Intact sorting, targeting, and clustering of γ-aminobutyric acid A receptor subtypes in hippocampal neurons in vitro. J Comp Neurol 443:43–55.

Chang BH, Mukherji S, Soderling TR (1998) Characterization of a calmodulin kinase II inhibitor protein in brain. Proc Natl Acad Sci U S A 95:10890–10895.

Churn SB, Sombati S, Jakoi ER, Severt L, DeLorenzo RJ, Sievert L (2000) Inhibition of calcium/calmodulin kinase II alpha subunit expression results in epileptiform activity in cultured hippocampal neurons. Proc Natl Acad Sci U S A 97:5604–5609.

Connolly CN, Wooltorton JR, Smart TG, Moss SJ (1996) Subcellular localization of γ-aminobutyric acid type A receptors is determined by β subunits. Proc Natl Acad Sci U S A 93:9899–9904.

DeLorey TM, Handforth A, Anagnostaras SG, Homanics GE, Minassian BA, Asatourian A, Fanselow MS, Delgado-Escueta A, Ellison GD, Olsen RW (1998) Mice lacking the $\beta 3$ subunit of the $GABA_A$ receptor have the epilepsy phenotype and many of the behavioural characteristics of Angelman syndrome. J Neurosci 18:8505–8514.

Farrant M, Brickley SG (2003) Properties of $GABA_A$ receptor-mediated transmission at newly formed Golgi-granule cell synapses in the cerebellum. Neuropharmacology 44:181–189.

Hájos N, Nusser Z, Rancz EA, Freund TF, Mody I (2000) Cell type- and synapse-specific variability in synaptic $GABA_A$ receptor occupancy. Eur J Neurosci 12:810–818.

Hamann M, Rossi DJ, Attwell D (2002) Tonic and spillover inhibition of granule cells controls information flow through the cerebellar cortex. Neuron 33:625–633.

Herd MB, Haythornthwaite AR, Rosahl TW, Wafford KA, Homanics GE, Lambert JJ, Belelli D (2008) The expression of $GABA_A$ beta subunit isoforms in synaptic and extrasynaptic receptor populations of mouse dentate gyrus granule cells. J Physiol 586:989–1004.

Houston CM, Smart TG (2006) CaMK-II modulation of $GABA_A$ receptors expressed in HEK293, NG108-15 and rat cerebellar granule neurons. Eur J Neurosci 24:2504–2514.

Houston CM, Lee HH, Hosie AM, Moss SJ, Smart TG (2007) Identification of the sites for CaMK-II-dependent phosphorylation of $GABA_A$ receptors. J Biol Chem 282:17855–17865.

Huntsman MM, Huguenard JR (2006) Fast IPSCs in rat thalamic reticular nucleus require the $GABA_A$ receptor $\beta 1$ subunit. J Physiol 572:459–475.

Ing T, Poulter MO (2007) Diversity of $GABA_A$ receptor synaptic currents on individual pyramidal cortical neurons. Eur J Neurosci 25:723–734.

Ives JH, Drewery DL, Thompson CL (2002) Differential cell surface expression of GABAA receptor $\alpha 1$, $\alpha 6$, $\beta 2$ and $\beta 3$ subunits in cultured mouse cerebellar granule cells influence of cAMP-activated signalling. J Neurochem 80:317–327.

Jones MV, Westbrook GL (1996) The impact of receptor desensitization on fast synaptic transmission. Trends Neurosci 19:96–101.

Jones MV, Westbrook GL (1997) Shaping of IPSCs by endogenous calcineurin activity. J Neurosci 17:7626–7633.

Kano M, Kano M, Fukunaga K, Konnerth A (1996) Ca^{2+}-induced rebound potentiation of γ-aminobutyric acid-mediated currents requires activation of Ca^{2+}/calmodulin-dependent kinase II. Proc Natl Acad Sci U S A 93:13351–13356.

Kawaguchi S-Y, Hirano T (2002) Signaling cascade regulating long-term potentiation of $GABA_A$ receptor responsiveness in cerebellar Purkinje neurons. J Neurosci 22:3969–3976.

Kittler JT, Moss SJ (2003) Modulation of $GABA_A$ receptor activity by phosphorylation and receptor trafficking: implications for the efficacy of synaptic inhibition. Curr Opin Neurobiol 13:341–347.

Laurie DJ, Seeburg PH, Wisden W (1992) The distribution of 13 $GABA_A$ receptor subunit mRNAs in the rat brain. II. Olfactory bulb and cerebellum. J Neurosci 12:1063–1076.

Leao RM, Mellor JR, Randall AD (2000) Tonic benzodiazepine-sensitive GABAergic inhibition in cultured rodent cerebellar granule cells. Neuropharmacology 39:990–1003.

Lisman J, Schulman H, Cline H (2002) The molecular basis of CaMK-II function in synaptic and behavioural memory. Nat Rev Neurosci 3:175–190.

Lüscher B, Keller CA (2004) Regulation of $GABA_A$ receptor trafficking, channel activity, and functional plasticity of inhibitory synapses. Pharmacol Ther 102:195–221.

McDonald BJ, Moss SJ (1994) Differential phosphorylation of intracellular domains of γ-aminobutyric acid type A receptor subunits by calcium/calmodulin type 2-dependent protein kinase and cGMP-dependent protein kinase. J Biol Chem 269:18111–18117.

McDonald BJ, Moss SJ (1997) Conserved phosphorylation of the intracellular domains of $GABA_A$ receptor $\beta 2$ and $\beta 3$ subunits by cAMP-dependent protein kinase, cGMP-dependent protein kinase protein kinase C and Ca^{2+}/calmodulin type II-dependent protein kinase. Neuropharmacology 36:1377–1385.

McDonald BJ, Amato A, Connolly CN, Benke D, Moss SJ, Smart TG (1998) Adjacent phosphorylation sites on $GABA_A$ receptor β subunits determine regulation by cAMP-dependent protein kinase. Nat Neurosci 1:23–28.

Moss SJ, Smart TG (1996) Modulation of amino acid-gated ion channels by protein phosphorylation. Int Rev Neurobiol 39:1–52.

Moss SJ, Gorrie GH, Amato A, Smart TG (1995) Modulation of $GABA_A$ receptors by tyrosine phosphorylation. Nature 377:344–348.

Nusser Z, Cull-Candy S, Farrant M (1997) Differences in synaptic $GABA_A$ receptor number underlie variation in GABA mini amplitude. Neuron 19:697–709.

Nusser Z, Hájos N, Somogyi P, Mody I (1998) Increased number of synaptic $GABA_A$ receptors underlies potentiation at hippocampal inhibitory synapses. Nature 395:172–177.

Nusser Z, Sieghart W, Mody I (1999) Differential regulation of synaptic $GABA_A$ receptors by cAMP-dependent protein kinase in mouse cerebellar and olfactory bulb neurones. J Physiol 521:421–435.

Nyíri G, Freund TF, Somogyi P (2001) Input-dependent synaptic targeting of $\alpha 2$-subunit-containing $GABA_A$ receptors in synapses of hippocampal pyramidal cells of the rat. Eur J Neurosci 13:428–442.

Pirker S, Schwarzer C, Wieselthaler A, Sieghart W, Sperk G (2000) $GABA_A$

receptors: immunocytochemical distribution of 13 subunits in the adult rat brain. Neuroscience 101:815–850.

Poisbeau P, Cheney MC, Browning MD, Mody I (1999) Modulation of synaptic $GABA_A$ receptor function by PKA and PKC in adult hippocampal neurons. J Neurosci 19:674–683.

Ponomarev I, Maiya R, Harnett MT, Schafer GL, Ryabinin AE, Blednov YA, Morikawa H, Boehm SL 2nd, Homanics GE, Berman AE, Berman A, Lodowski KH, Bergeson SE, Harris RA (2006) Transcriptional signatures of cellular plasticity in mice lacking the α1 subunit of $GABA_A$ receptors. J Neurosci 26:5673–5683.

Rossi D, Hamann M (1998) Spillover-mediated transmission at inhibitory synapses promoted by high affinity α6 subunit $GABA_A$ receptors and glomerular geometry. Neuron 20:795.

Rudolph U, Möhler H (2004) Analysis of $GABA_A$ receptor function and dissection of the pharmacology of benzodiazepines and general anesthetics through mouse genetics. Annu Rev Pharmacol Toxicol 44:475–498.

Shen K, Meyer T (1999) Dynamic control of CaMKII translocation and localization in hippocampal neurons by NMDA receptor stimulation. Science 284:162–166.

Shen K, Teruel MN, Connor JH, Shenolikar S, Meyer T (2000) Molecular memory by reversible translocation of calcium/calmodulin-dependent protein kinase II. Nat Neurosci 3:881–886.

Singleton MW, Holbert WH 2nd, Ryan ML, Lee AT, Kurz JE, Churn SB (2005) Age dependence of pilocarpine-induced status epilepticus and inhibition of CaM kinase II activity in the rat. Brain Res Dev Brain Res 156:67–77.

Sur C, Wafford KA, Reynolds DS, Hadingham KL, Bromidge F, Macaulay A, Collinson N, O'Meara G, Howell O, Newman R, Myers J, Atack JR, Dawson GR, McKernan RM, Whiting PJ, Rosahl TW (2001) Loss of the major $GABA_A$ receptor subtype in the brain is not lethal in mice. J Neurosci 21:3409–3418.

Thomas P, Mortensen M, Hosie AM, Smart TG (2005) Dynamic mobility of functional $GABA_A$ receptors at inhibitory synapses. Nat Neurosci 8:889–897.

Thompson SA, Wheat L, Brown NA, Wingrove PB, Pillai GV, Whiting PJ, Adkins C, Woodward CH, Smith AJ, Simpson PB, Collins I, Wafford KA (2004) Salicylidene salicylhydrazide, a selective inhibitor of β1-containing $GABA_A$ receptors. Br J Pharmacol 142:97–106.

Wang Q, Liu L, Pei L, Ju W, Ahmadian G, Lu J, Wang Y, Liu F, Wang YT (2003) Control of synaptic strength a novel function of Akt. Neuron 38:915–928.

Wang RA, Kolaj CM, Randic M (1995) α-Subunit of calcium/calmodulin-dependent protein kinase II enhances γ-aminobutyric acid and inhibitory synaptic responses of rat neurons i*n vitro.* J Neurophysiol 73:2099–2106.

Weeber EJ, Jiang Y-H, Elgersma Y, Varga AW, Carrasquillo Y, Brown SE, Christian JM, Mirnikjoo B, Silva A, Beaudet AL, Sweatt JD (2003) Derangements of hippocampal calcium/calmodulin-dependent protein kinase II in a mouse model for Angelman mental retardation syndrome. J Neurosci 23:2634–2644.

Wei W, Zhang N, Peng Z, Houser CR, Mody I (2003) Perisynaptic localization of δ subunit-containing $GABA_A$ receptors and their activation by GABA spillover in the mouse dentate gyrus. J Neurosci 23:10650–10661.